

Supplementary Material for
Surface/interfacial of pores desalination mechanisms revealed
through 2D carbon-based membranes

Xiaoyang Zhao^a, Kun Meng^{a,*}, Yutao Niu^a, Sen Ming^a, Ju Rong^a, Xiaohua Yu^a,

Yannan Zhang^b

^aFaculty of Materials Science and Engineering, Kunming University of Science and
Technology, Kunming, 650093, China.

^bNational and Local Joint Engineering Laboratory for Lithium-ion Batteries and
Materials Preparation Technology, Kunming University of Science and Technology,
Kunming 650093, China.

E-mail addresses: mkkmust@163.com

S1. The Structure Concept of UWY-style IM-20 Zeolite

IM-20 was hydrothermally synthesized from a gel prepared by mixing Aerosil 200 (>98% Degussa), amorphous germanium oxide GeO_2 (>99.99%, Aldrich), HF acid (40%, Carlo Erba), distilled water, and 3-butyl-1-methyl-3H-imidazol-1-ium bromide (98%, Solvionic), which had previously been transformed into its OH form by ion exchange in water (Dowex SBR LC NG, OH Form (Supelco)). The gel composition was $0.6 \text{ SiO}_2:0.4 \text{ GeO}_2:0.5 \text{ OSDA}(\text{OH}):0.5 \text{ HF}:10 \text{ H}_2\text{O}$ ($\text{pH} \approx 8$). The structure of IM-20 was solved from a synchrotron powder X-ray diffraction pattern of the calcined product. It was indexed in an orthorhombic unit cell with $a = 25.165(6) \text{ \AA}$, $b = 12.701(2) \text{ \AA}$, and $c = 11.601(1) \text{ \AA}$ using the indexing algorithms DICVOL. The analysis of the systematic extinctions suggested the possible space groups $P222$ (No. 16), $Pmm2$ (No. 25), or $Pmmm$ (No. 47). The crystal structure was then solved by direct methods applied on the extracted intensities using the program EXPO2004 with the highest symmetry ($Pmmm$) and refined with the GSAS package.

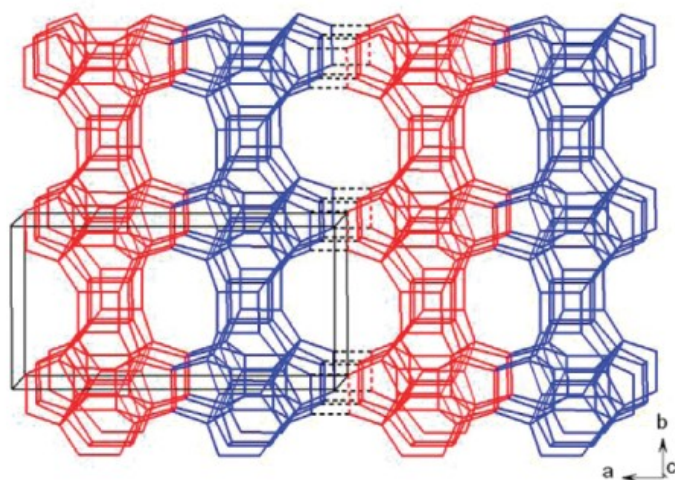


Fig. S1. Building scheme of IM-20 ([001] crystal plane).

Reference

M. Dodin, J.L. Paillaud, Y. Lorgouilloux, P. Caullet, E. Elkaim, N. Bats, A zeolitic material with a three-dimensional pore system formed by straight 12-and 10-ring channels synthesized with an imidazolium derivative as structure-directing agent, J. Am. Chem. Soc. 132 (30) (2010) 10221-10223.

S2. Structural Screening

S2.1 Data preparation

All structural data of the 2D zeolite-like carbon materials were obtained by applying the CALYPSO structure prediction method developed by Ma's group, which is grounded on the ML particle swarm optimization algorithm to explore and predict functional materials on demand. In the structural prediction, the number for the C atom in one formula unit was 12, and the maximum number of formula units per cell was 2. Also, the primary estimated volume per formula unit was 20 Å³ and the prediction generation was 50. In addition, the population size of the predicted structures was 40 in every generation, and the proportion of randomly generated structures in each generation was 40%. It should be noted that our CALYPSO crystal structure prediction method was interfaced with the Vienna ab initio simulation package (VASP), and each generated structure was optimized thrice to ensure accurate calculation.

S2.2. Machine learning models

Enriching the π -bonds and building multiple carbon ring structures rationally should be an active solution to regulate the mechanical properties and electronic

structure. All data of the original dataset were split into 70% training and 30% test sets. The training set was used to optimize and train the model through cross-validation, while the test set was employed to evaluate the accuracy of the trained model. We trained each ML model utilizing a 5-fold cross-validated grid search to optimize the hyperparameters, i.e., dividing the data into five random groups and training the model with four of the five subsets, then evaluating the remaining subsets. The process was repeated for each of the five divisions as the test set, after which the predictive ability of the model was evaluated as the average performance of the model over all replications. This is done so that each segmented dataset is treated as a test set for the iteration. Neural networks (NN) have been extensively applied for predicting material properties and accelerating simulation to assist material characterization due to their advantages of self-learning, associative storage, and the ability to find optimization solutions at high speed. Numerical features such as energy density, adsorption energy, and mechanical properties were renormalized and served as the input feature vectors for the NN model. The correlation between the energy density and the pore size features of 2D membranes was first established using the NN model, which consists of an input layer, an output layer, and two totally connected hidden layers, and the size of the hidden layers was determined by applying the grid search method. Among them, the input characteristics of the NN input layer are $E \leq -8.5$ eV/atom. In addition, we have selected the layer magnitude parameter set to 100 for the hidden layers. The mean squared errors and the rectified linear unit were adopted as the lost function and activation function, respectively. The root mean absolute error

(MAE) of the test set measured on the model was 0.27%, and the coefficient of determination (R^2) value was 0.95. Based on the similar operation described above, the adsorption energy and mechanical properties of the suitable pore size were further screened (the input characteristics of the NN input layer were $U < -0.5$ eV and $C(\theta) > 32$ GPa and $\nu(\theta) > 0.25$, respectively).

S2.3 Structural screening

Some crucial eigenvectors are considered during training: (i) The total energy released by forming the structure is applied as a physical parameter to determine the structural stability. The criterion for obtaining a stable structure is defined as the total energy $E \leq -8.5$ eV/atom after referring to the stability of numerous graphene-based materials; (ii) The pore size is an essential indicator for desalination properties. According to previous studies, a pore size of 0.45–0.55 nm can display excellent desalination efficiency, and the corresponding carbon rings in the carbon density model should contain 10–12 carbon atoms; (iii) To ensure the strength and integrity of the structure during desalination, the Young's modulus C and Poisson's ratio ν act as descriptors of the mechanical properties, and the screening terms are set to $C(\theta) > 32$ GPa and $\nu(\theta) > 0.25$; (iv) The best-fitting algorithm for the training set is employed to predict the adsorption energy of a Na^+ at a hollow site. For stable adsorption, the screening judgment of $U < -0.5$ eV is performed empirically; (v) Finally, we have to evaluate the preparation possibilities of the structures. The determination criteria for the structural screening are shown in Fig. S2.

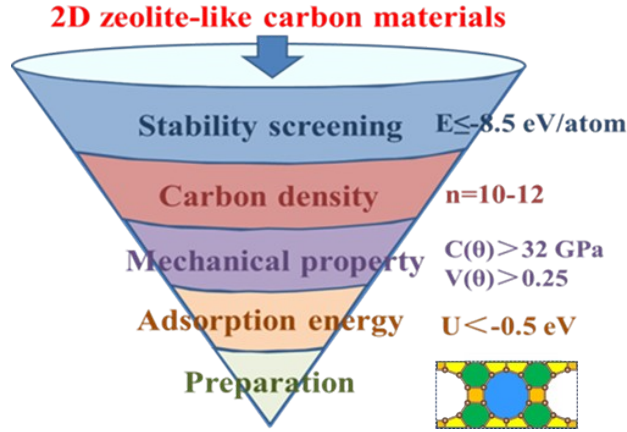


Fig. S2. Determination criteria for structural screening.

Specifically, the stability screening data are plotted in Fig. S3. The magenta line indicates $E = -8.5$ eV/atom, whereas the blue and red dots represent the structure subsets that do not fulfill and satisfy the screening criteria in the unit cell, respectively. We treated 292 2D carbon nanomaterials and obtained 52 target spots ($E \leq -8.5$ eV/atom) according to the stability criteria, which can be assumed as stable unit cells to be further investigated.

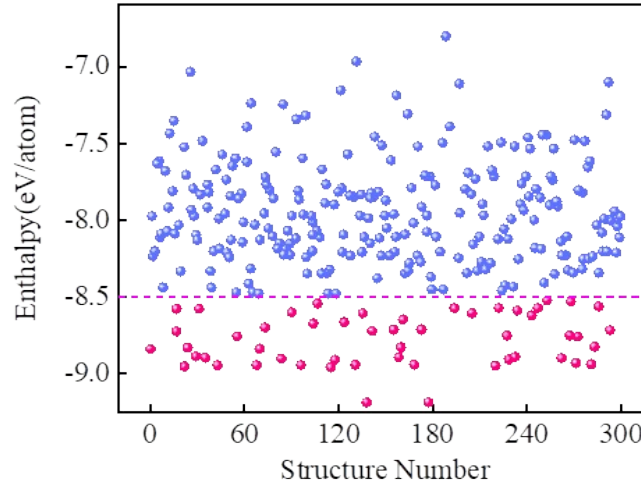


Fig. S3. Stability screening of machine learning.

Fig. S4 illustrates the correspondence between carbon density and total energy of feasible stable structures. They are based on the constructed carbon density model

used to further search for the structures that match the screening eligibility. The structures of the largest pores, containing 7–9, 10–12, and 14–18 carbon atoms in the unit cell, are represented with yellow, red, and blue dots, respectively. The energy values corresponding to the pore structures constructed with different amounts of carbon atoms are further summarized in the embedded diagram. We searched for some stable structures incorporating 10- to 12-membered carbon rings, where the 10-membered carbon ring structures have energies in the range of -8.372 to -8.830 eV/atom. Similarly, the 12-membered carbon ring structures have energy values between -8.501 and -8.600 eV/atom.

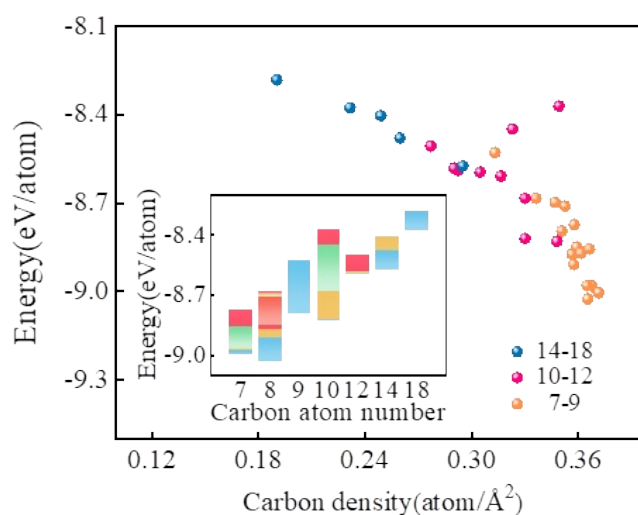


Fig. S4. Correspondence between carbon density and total energy.

These structures have been further screened for mechanical properties and adsorption energy. Finally, based on the results of the screening, a main target was chosen for subsequent simulation validation in this paper to explore the universal characteristics of desalination membrane structures. Therefore, ML provides a possible solution for developing 2D carbon membranes for seawater desalination.

S3. Classical Molecular Dynamics

S3.1 Seawater desalination system model

All the molecular dynamics simulations were carried out using the LAMMPS package. The SPE/C water model was adopted for the explicit solvent. The long-range electrostatic interactions were treated by the Particle Mesh Ewald method, and a typical distance cutoff of 12 Å was used for the van der Waals interactions. The non-bonded interaction pair list was updated every 10 fs. In order to place strain on the Carzeo-ANG filter, the cross section along the x-y plane in the simulation box was fixed at a certain value. Canonical sampling was performed through the velocity rescaling method at constant temperature of 1000 K. An integration time step of 1 fs was used for all simulations. The simulation box contains 4467 water molecules, 80 Na⁺, 80 Cl⁻, a Carzeo-ANG filter, and an ideal single graphene sheets used as a piston. The system was firstly equilibrated with z-direction pressure coupling at 1atm for 10 ns, followed by 30 ns productive simulations under a given constant piston pressure in the otherwise NVT ensemble.

S3.2 Script of ions movement in the electric field

```
#!/perl

use strict;

use Getopt::Long;

use MaterialsScript qw(:all);

my $doc = $Documents{"packmol- Carzeo-ANG.xsd"};

Modules->Forcite->ChangeSettings([
```



```

        ElectricFieldStrength => 1,

        ElectricFieldX => 0,

        ElectricFieldY => 0,

        ElectricFieldZ => 1,

        CounterElectricField =>"No"]);

my $results = Modules->Forcite->Dynamics->Run($doc, Settings(

    Quality => 'Medium',

    CurrentForcefield => 'Universal',

    ChargeAssignment => 'Use current',

    Ensemble3D => 'NVT',

    TrajectoryFrequency => 100,

    AssignFixedBonds => 'No'));

my $outTrajectory = $results->Trajectory;

my $results = Modules->Forcite->Dynamics->Run($doc, Settings(

    ChargeAssignment => 'Use current',

    Ensemble0D => 'NVT',

    Ensemble3D => 'NVT',

    Temperature => 300,

    NumberOfSteps => 8000,

    TrajectoryFrequency => 8000));

my $outTrajectory = $results->Trajectory;

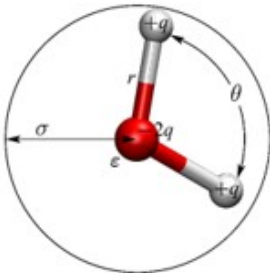
```

S3.3 SPC/E model and force field parameter

(1) LJ potential calculation formula :

$$U = \sum_i \sum_{j>i} 4\epsilon_{ij} \left[\left(\frac{\sigma_{ij}}{r_{ij}} \right)^{12} - \left(\frac{\sigma_{ij}}{r_{ij}} \right)^6 \right] + \sum_i \sum_{j>i} k \frac{q_i q_j}{r_{ij}}$$

Table S1. Parameters of SPC/E model for water molecules

Parameters	Values	SPC/E water molecule model
ϵ (kcal/mol)	-0.1553	
σ (Å)	3.166	
R (Å)	1	
θ (°)	109.47	
q (q)	(±)0.4238	

(2) Core code :

Mass :

Ow 15.9994

Hw 1.008

Charge :

Ow -0.8476

Hw 0.4238

pair_style lj/cut/coul/long 9.0

pair_coeff 1 1 0.1553 3.166 # 1=Ow, 2=Hw

pair_coeff 1 2 0 0

pair_coeff 2 2 0 0

bond_style harmonic

bond_coeff 1 0.0 1.0 # 1=Ow-Hw

angle_style harmonic

angle_coeff 1 0.0 109.47 # 1=Hw-Ow-Hw

kpace_style ppm 1.0e-4

fix 1 watergroup shake 0.0001 20 0 b 1 a 1

(3) LJ potential parameters

The parameters are summarized in Table S2.

Table S2. LJ and charge parameters employed in this work

Element	C _{piston}	C _{Carzo-ANG}	H _w	O _w	Cl ⁻	Na ⁺
ε(kcal/mol)	0.1050	0.1050	0.0	0.1553	0.0128	0.3526
σ(Å)	3.8510	3.8510	0.0	3.1656	2.1600	4.8305
q(e)	0.0	0.0	0.4238	-0.8476	-1.00	1.00

S3.4 Applied pressures of other 2D materials

Table S3. The pressure values required to achieve 100% salt rejection for other materials

References	Materials	Pressure (MPa)
[1]	Nanoporous graphene	125
[2]	Graphene kirigami	100
[3]	Carbon nanocones (CNCs)	100
[4]	Single-layer Metal-Organic Framework Membranes	100
[5]	Nanoporous graphitic carbon nitride membranes	60
[6]	Nanoporous Boron Nitride Nanosheet Membranes	50
[7]	layer-stacked black phosphorus carbide (α -PC) membrane	40
[8]	Carzo-ANG membranes	65

[1] Nano Letters, 2012, 12(7): 3602-3608.

[2] Carbon, 2022, 195: 183-190.

- [3] Carbon, 2018, 129: 374-379.
- [4] Nano Letters, 2019, 19(12): 8638-8643.
- [5] Journal of Membrane Science, 2021, 620: 118869.
- [6] The Journal of Physical Chemistry C, 2017, 121(40): 22105-22113.
- [7] Desalination, 2022, 522: 115422.
- [8] This work.”

S4. The Self-cleaning Property of Carzeo-ANG

S.4.1 The calculations of the self-cleaning property

Simulation were carried out by Forcite module of commercially available software Materials Studio (Accelrys Software Inc.). Forcite do not support such kind of calculation (Applying an electric field in modelled structures) but it has embedded PERL interpreter. Thus, the procedure of simulation combined with the electric field was carried out by PERL script language. In order to describe interatomic bonds and non-bonding potential energy, the ClayFF force field was used for simulations. Next, the structures were equilibrated by thermostat at desired temperature (300 K) during 100 fs. Such time is required to achieve uniform temperature distribution for the model, time step of simulation was set at 1 fs. The NVT ensemble was used at the next step. From this moment to the end of simulation (till 10 ps) at every time step (1 fs) and the constant value (1 V/Å), electric field strength was added along the electric field direction vector Z component.

S5. The POSCAR file of Carzeo-ANG

Carzeo-ANG

1.0000000000000000

12.7897794267706022	-0.0014983097560707	0.0000000000000000
-0.0007218867179829	6.2188773745001278	0.0000000000000000
0.0000000000000000	0.0000000000000000	15.0000000000000000

C

26

Direct

0.0583690749277821	0.8835446296423228	0.5000000000000000
0.1619635857713106	0.8040501791464365	0.5000000000000000
0.2218146578373918	0.6158500334573773	0.5000000000000000
0.2218653904158643	0.3838751486153740	0.5000000000000000
0.1620703074375669	0.1956064359267771	0.5000000000000000
0.0584585974578928	0.1163624914750727	0.5000000000000000
0.2248554205142170	0.9998028316789984	0.5000000000000000
0.3316036572067205	0.9999073858442813	0.5000000000000000
0.3950375205765866	0.8068434661019666	0.5000000000000000
0.3374807806937383	0.6177866109161627	0.5000000000000000
0.3374844560673651	0.3821366112602576	0.5000000000000000
0.3949981592564455	0.1931092891184036	0.5000000000000000
0.5009574613050489	0.1163084820898703	0.5000000000000000

0.5009757655245082	0.8839611939582284	0.5000000000000000
0.6703496820333186	0.0003415721766871	0.5000000000000000
0.6069268688040452	0.8071745009688129	0.5000000000000000
0.6644193012995530	0.6181029093108705	0.5000000000000000
0.6644289802712890	0.3824686874062664	0.5000000000000000
0.6068901690883450	0.1933829272946070	0.5000000000000000
0.7770995507107656	0.0004354574310312	0.5000000000000000
0.8399886288027432	0.1962144309348730	0.5000000000000000
0.7801066210417105	0.3844022174504573	0.5000000000000000
0.7800499642444407	0.6163488970826165	0.5000000000000000
0.8398694329382508	0.8045980386127241	0.5000000000000000
0.9434658505214770	0.8838391798087315	0.5000000000000000
0.9435600872516545	0.1166864982907967	0.5000000000000000

S6. AIMD simulation at 300 K

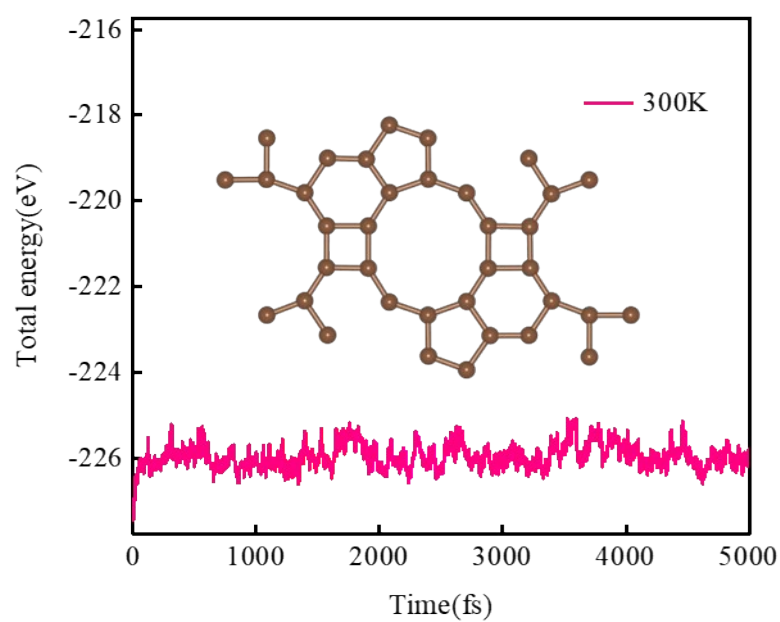


Fig. S5 total potential energy fluctuation of Carzeo-ANG during AIMD simulation at 300 K

S7. Adsorption properties of Cl^-

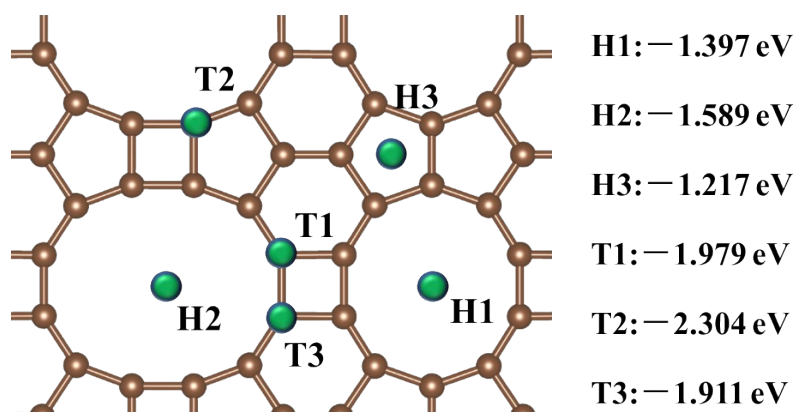


Fig. S6 Adsorption model and adsorption energies at different sites of Cl^-

Dynamic simulation of seawater desalination

See Appendix 1.